MECHANISM OF FOAM DESTRUCTION BY EMULSIONS OF PDMS-SILICA MIXTURES

Nikolai D. Denkov,[1]* *Krastanka Marinova,*[1] *Slavka Tcholakova,*[1]

and Martial Deruelle[2]

[1]Laboratory of Chemical Physics & Engineering,

Faculty of Chemistry, Sofia University, 1164 Sofia, Bulgaria

[2]Rhodia Silicones Europe, 55 rue des Freres Perret, BP 22, F-69191, Saint-Fons Cedex, France

*Correspondence:
Dr. Nikolai Denkov
Laboratory of Chemical Physics & Engineering
Faculty of Chemistry, Sofia University
1 James Bourchier Ave., 1164 Sofia
Bulgaria

Phone: (+359-2) 962 5310
Fax: (+359-2) 962 5643
E-mail: ND@LCPE.UNI-SOFIA.BG

Keywords: antifoams, defoamers, PDMS, silicone oil, PDMS-silica mixture

ABSTRACT

Emulsions of oil-silica mixtures are used for foam control in various technological applications and consumer products. PDMS-silica mixtures are particularly efficient as foam breakers – typically, they destroy the foam within seconds and are sometimes termed "the fast antifoams". Recent studies revealed that the foam destruction by PDMS-silica mixtures occurs through the so called "bridging-stretching mechanism" of foam film rupture. The experiments showed also that the antifoam emulsions gradually loose their antifoam activity in the course of foam destruction by a mechanism, which was explained elsewhere. In this study we suggest a phenomenological model for description of the antifoam performance of the fast antifoams. This model includes three parameters for characterization of the antifoam properties: one of these parameters characterizes the initial antifoam activity, whereas the other two characterize the antifoam durability. The parameters are chosen in such a way, as to depend slightly on the particular foam test, used to characterize the antifoam properties. The model is supported by several experiments with two different foam tests.

1/ Introduction.

Emulsions of oil-silica mixtures are widely used for foam control in various technological applications and consumer products (1). The mixtures of hydrophobic silica and silicone oil (PDMS) are particularly efficient as foam breakers and usually destroy the foam within seconds - that is why they were termed "the fast antifoams" (2). Recent studies revealed that the foam destruction by emulsions of such PDMS-silica mixtures occurs through the so called "bridging-stretching mechanism" (3,4). According to this mechanism, the antifoam globules form capillary-unstable oil bridges between the two surfaces of the foam films. These bridges rapidly stretch in radial direction, due to uncompensated capillary pressures across the oil-water and oil-air interfaces, and eventually rupture, destroying in this way the foam films. Observations by a high-speed video camera showed that usually one antifoam globule is responsible for the rupture of one foam film (3).

The experiments show that the antifoam emulsions gradually loose their activity in the course of foam destruction (5). This process has been explained by a segregation of the antifoam globules into two inactive populations: silica-enriched globules and silica-deprived globules. The silica enriched globules are unable to destroy the foam films, because they behave as non-deformable entities and the formed bridges between the foam film surfaces cannot stretch (i.e. the bridging-stretching process cannot be accomplished). On the other hand, the silica-deprived globules are inactive, because their entry barrier is so high that no oil bridges are formed in the foam films (6). As a final result, most of the antifoam globules become inactive in the process of foam destruction and the antifoam is considered as being exhausted (deactivated).

On the basis of our current understanding of the mechanisms of antifoam action and exhaustion (3-5), we suggest in the present study a phenomenological model for description of the antifoam performance of PDMS-silica mixtures. This model includes three parameters for characterization of the antifoam properties: one of these parameters characterizes the initial antifoam activity, whereas the other two characterize the antifoam durability. These parameters are chosen in such a way, as to depend slightly on the particular foam test, used to characterize the antifoam properties. The relevance of the theoretical model to real systems has been demonstrated by analyzing the results from experiments performed with two different foam tests.

2/ Materials and Methods.

Sodium bis(2-ethylhexyl) sulfosuccinate (Sigma catalogue No D-0885; named hereafter AOT) is used as a surfactant. Its concentration in the working solutions is 10 mM, which is about 3.5 times the critical micellar concentration, CMC=2.8 mM. All solutions are prepared with doubly distilled water.

Two antifoam substances are studied:

(1) *Compound A* (CA) consists of PDMS oil 47V1000SH (product of Rhodia Silicones; viscosity 1000 cP) containing 4.2 wt % hydrophobized silica particles R974 of pyrogenic origin with a specific surface area of approx. 200 m^2/g (Degussa). The dispersion of this silica in silicone oil leads to formation of agglomerates, which have a fractal structure and broad size distribution, from 0.1 to 5 μm.

(2) *Emulsion A* (EA) is a 10 wt % aqueous emulsion of Compound A, which is further diluted to the desired final concentration in the surfactant solution. The stock emulsion is stabilized by two non-ionic surfactants (sorbitan monostearate – Span 60, and ethoxylate of stearic acid with 40 ethoxy groups – stearyl-EO_{40}). Microscope observations show that this emulsion is relatively polydisperse with drop diameters ranging from ca. 1 to 10 μm.

The antifoam concentration in the working solutions was 0.01 or 0.02 wt % (defined as the mass of silicone oil over the mass of the working solution).

Two foam tests were used for characterization of the antifoam performance:

Foam Rise Method (bubble generation by using a bunch of capillaries). 100 mL of the surfactant solution is poured in a standard 550 mL glass cylinder of 37 mm internal diameter. A bunch of 27 glass capillaries (internal diameter 0.13 mm) is mounted at the bottom of the cylinder. Monodisperse foam bubbles of diameter ≈ 3 mm are generated by blowing nitrogen gas at constant flow

rate through these capillaries. The foam volume is measured as a function of time in the absence of antifoam (to determine the foam generation rate) and after the introduction of antifoam (to determine the antifoam activity and durability). The test ends when the generated foam fills up the cylinder. In this test, longer time needed for filling up the cylinder corresponds to better antifoam durability.

Automatic Shake Test (*AST*): 100 mL of the surfactant solution is poured in a standard 250 mL glass jar and the antifoam is afterward added. The jar is shaken on a shake-machine Agitest (Bioblock) at a frequency of 360 min^{-1} and an amplitude of 2 cm for a given period of time. After each cycle of agitation, the solution remains quiescent for another 60 s. During this period, the defoaming time, τ_D, is measured – it is defined as the time for appearance of a clean water-air interface without bubbles. Afterwards, a new shaking cycle is performed and this procedure is repeated until the defoaming time exceeds 60 s in three consecutive cycles. In this way, τ_D is determined as a function of the number of the shaking cycle, N, or as a function of the total foaming time, t (which is a product of the number of the cycle and the duration of one cycle). Longer total foaming time before the compound exhaustion corresponds to better antifoam durability and vice versa.

3/ Phenomenological model for description of the antifoam activity and durability.

3.1. Main experimental observations and formulation of the model. The experiments with various fast antifoams (silica-PDMS mixtures) showed that, typically, the antifoam has high initial activity, which gradually decreases during the process of foam destruction. However, this initial decrease of the antifoam activity is relatively slow and the antifoam remains rather active for a certain period of time (Stage 1). After this period, whose duration strongly depends on the antifoam concentration, a sudden, almost complete loss of the antifoam activity is observed, which is evidenced by the rapid foam growth in the test (Stage 2). This typical behavior is illustrated in Figure 1 with results from the two foam tests, used by us. In figure 1A, one observes a sharp break in the curve foam volume vs. foaming time in the foam rise test. The moment of this break is denoted by t^* in Figure 1A. Similarly, in Figure 1B we see a break, denoted by N^*, in the curve showing the defoaming time as a function of the number of foaming cycles. In both cases, this break indicates the moment of antifoam exhaustion, i.e. the transition from Stage 1 to Stage 2.

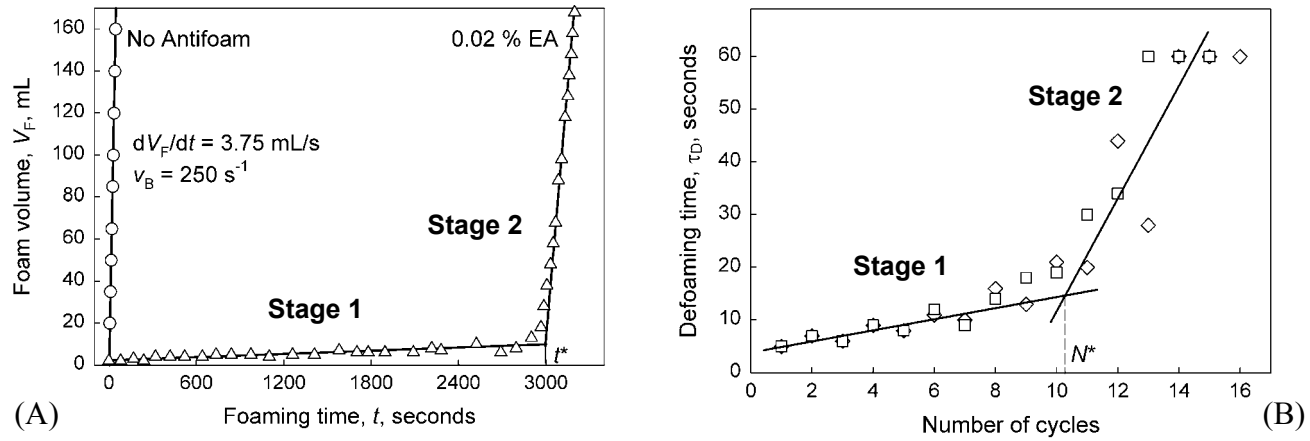

Figure 1.Typical results from the foam tests with 10 mM AOT solutions containing 0.02 wt % of Emulsion A: (A) Foam rise method; (B) Automatic shake test; the duration of one shake cycle is 30 s.

Let us consider first the foam rise method (Figure 1A). Note that the dynamics of foam generation and destruction in this test is similar to that in the so called Ross-Miles test, which is widely used as a standard foam test in the research and application laboratories. Therefore, the consideration presented below is applicable without any significant modification to the Ross-Miles test, as well.

The foaming rate, (dV_F/dt), is measured in the absence of antifoam. From the foaming rate and the size of the bubbles, one can calculate the rate of bubble production, v_B (number of bubbles per unit

time), during the experiment

$$\mathrm{v}_B = \frac{1}{V_B}\frac{\mathrm{d}V_F}{\mathrm{d}t} \qquad [1]$$

where V_B is the mean volume occupied by one bubble in the foam column (V_B is practically equal to the mean bubble volume). For the experiment shown in Figure 1A, $\mathrm{d}V_F/\mathrm{d}t \approx 3.75$ mL/s, $V_B \approx 0.015$ mL and, subsequently, $\mathrm{v}_B \approx 250$ bubbles per second.

In the presence of antifoam, a fraction of these newly created bubbles coalesce with each other and with the atmosphere above the foam column. The initial antifoam concentration at the beginning of the foam test is C_{A0}. In the course of foam destruction, the concentration of the active antifoam, $C_A(t)$, gradually decreases due to the antifoam exhaustion. Correspondingly, the concentration of the bubbles, $C_B(t)$, slowly increases. These changes can be quantified by a set of two kinetic equations for the concentrations of the bubbles and of the active antifoam, respectively

$$\frac{\mathrm{d}C_B}{\mathrm{d}t} = \mathrm{v}_B - k_1 C_A C_B \qquad [2]$$

$$\frac{\mathrm{d}C_A}{\mathrm{d}t} = -k_2 C_A C_B \qquad [3]$$

The constant k_1 in Eq. 2 characterizes how active is the antifoam with respect to bubble destruction, viz. k_1 characterizes the antifoam activity. As shown below, the antifoam durability is characterized by the ratio k_2/k_1.

A particular feature of Stage 1 is that the rate of bubble formation is practically equal to the rate of bubble destruction, which is evidenced by the fact that the foam volume during the entire Stage 1 remains very small. Therefore, one can use the following steady-state approximation to describe the processes during Stage 1:

$$\frac{\mathrm{d}C_B}{\mathrm{d}t} \approx 0 \qquad \text{(Stage 1)} \qquad [4]$$

which, according to Eq. 2, is equivalent to

$$k_1 C_A C_B \approx \mathrm{v}_B = \text{const.} \qquad \text{(Stage 1)} \qquad [4']$$

Therefore, Eq. 3 can be represented in the form

$$\frac{\mathrm{d}C_A}{\mathrm{d}t} = -\frac{k_2}{k_1}\mathrm{v}_B = \text{const.} \qquad \text{(Stage 1)} \qquad [5]$$

The set of Eqs. 4' and 5 has the following explicit solution:

$$C_B(t) \approx \frac{\mathrm{v}_B}{k_1\left(C_{A0} - k_3 t\right)} = \frac{1}{\left(k_1/\mathrm{v}_B\right)C_{A0} - k_2 t} \qquad \text{(Stage 1)} \qquad [6]$$

$$C_A(t) \approx C_{A0} - k_3\, t \qquad \text{(Stage 1)} \qquad [7]$$

where k_3 is defined through the expression

$$k_3 \equiv \frac{k_2}{k_1} \mathrm{v}_B \qquad [8]$$

As seen from Eqs. 7 and 8, k_3 presents the rate of antifoam exhaustion, which is proportional to the rate of bubble generation (viz., on the foaming method). It is more practical to characterize the antifoam exhaustion by the ratio k_2/k_1, which should slightly depend on the particular foaming method.

The onset of Stage 2 indicates the moment, when the rate of bubble destruction becomes insufficient to compensate the process of bubble formation and, as a result, the foam volume starts increasing rapidly with time. This result means that there is a critical concentration of antifoam, C_A^*, below which the antifoam is unable to suppress efficiently the foam generated in the test. In other words, Eqs. 4 to 7 are not satisfied at $C_A < C_A^*$. One may expect that the value of C_A^* should not depend on the initial antifoam concentration, C_{A0}, for a given foam test and surfactant-antifoam couple.

Let us note that the relevant, experimentally accessible quantities are the initial antifoam concentration, C_{A0}, and the time, t^*, corresponding to the end of Stage 1 (viz. the moment when the steady-state approximation is violated). Equation 7 suggests that C_{A0}, and t^* are interrelated for a given system by the equation:

$$t^*\left(C_{A0}\right) = \frac{1}{k_3}\left(C_{A0} - C_A^*\right) \qquad \text{(end of Stage 1)} \qquad [9]$$

Therefore, the model predicts that the plot of t^* vs. C_{A0} should be a linear function. From the slope and the intersect of this dependence one could determine k_3 and C_A^*. Finally, from the values of k_3, C_A^*, and $C_B^* \equiv C_B(t=t^*)$ one can determine the constants k_1 and k_2 (see Eqs. 4' and 8):

$$k_1 = \frac{\mathrm{v}_B}{C_A^* C_B^*} \qquad \text{(end of Stage 1)} \qquad [10]$$

$$k_2 \equiv \frac{k_3 k_1}{\mathrm{v}_B} \qquad [11]$$

where C_B^* is preferably taken as an average value from the series of experiments at different C_{A0}. This procedure may encounter difficulties if the value of C_A^* is very small and is determined with low accuracy. In this case, k_3 can be estimated from experiments at a single antifoam concentration:

$$k_3 \approx C_{A0} / t^* \qquad (C_A^* << C_{A0}) \qquad [9']$$

If this approximation is used, then Eq. 10 cannot be used to determine k_1. Instead, one can determine k_1 from the initial antifoam and bubble concentrations:

$$k_1 = \frac{\mathrm{v}_B}{C_{A0} C_{B0}} \qquad (t = 0) \qquad [12]$$

One should note, however, that the bubble concentration at the very beginning of the experiment, C_{B0}, is typically low and is often measured with poor accuracy. As a result, the determination of k_1 through Eq. 12 may be not very accurate. In other words, one should chose between Eqs. 10 and 12 for data interpretation, depending on the accuracy of determination of C_A^* and C_{B0}.

The above consideration implies that the antifoam performance can be characterized by three parameters: k_1 (characterizing the antifoam activity), and k_2/k_1 and C_A^* (both characterizing the antifoam durability). If $C_A^* << C_{A0}$, it might be convenient to characterize the antifoam durability by the quantity:

$$Dr = \frac{\mathrm{v}_B\, t^*}{C_{A0}} = \frac{k_1}{k_2} \qquad \text{(durability measure, } C_A^* << C_{A0}\text{)} \qquad [13]$$

which is equal to the number of bubbles destroyed by the antifoam before its exhaustion, normalized by the antifoam concentration. Note that Dr is easily determined from the experiment and should not depend on C_{A0} and v_B in the framework of the current model. Under the same assumptions, the constant k_1, which characterizes the antifoam activity can be found from the experiment through Eq. 14, which is obtained by averaging Eq. 4' over the entire period of Stage 1:

$$k_1 = \frac{2\mathrm{v}_B}{C_{A0}\langle C_B \rangle} \qquad \text{(activity measure, } C_A^* << C_{A0}\text{)} \qquad [14]$$

Here $<C_B>$ indicates the average concentration of bubbles during Stage 1. Such an averaging smooths down the appreciable fluctuations in the foam volume (viz. in $C_B(t)$) during Stage 1, as a result of the stochastic nature of the bubble coalescence.

Let us note at the end of this section that the above equations can be applied to the periodic shake test, as described in Section 2, if one considers t as being the actual foaming time (number of shake cycles multiplied by the duration of one cycle). The rapid increase of the defoaming time in these experiments indicates the end of Stage 1 – the antifoam becomes unable to destroy the bubbles generated during one shaking cycle (the steady-state approximation is violated). One difficulty in the application of the proposed model to the shake test is that the rate of bubble generation, v_B, is not easily determined – the generated bubbles are very polydisperse and the foam rapidly fills up the jar containing the foaming solution. As a result, the value of v_B is usually unknown or can only be roughly estimated. If v_B is not known, one can determine the ratio k_1/v_B from the experimental data.

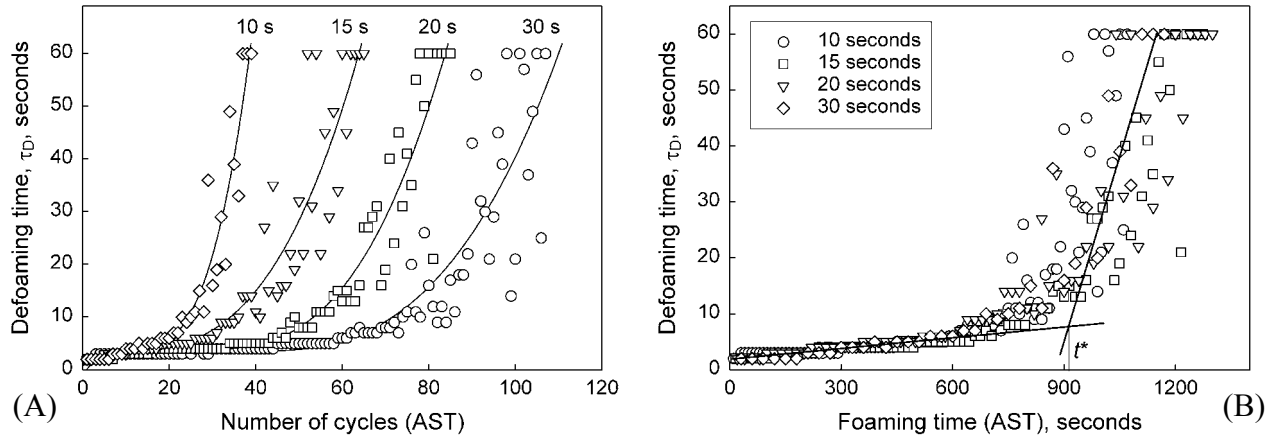

Figure 2. Defoaming time for 10 mM AOT solutions in the presence of 0.01 wt % of Compound A at different durations of one shaking cycle (10, 15, 20, or 30 s) as a function of: (A) Number of shaking cycles; (B) Total foaming time. Note that the different curves from (A) fall in a single master curve in (B).

3.2. Some illustrative results. The main purpose of this section is to demonstrate the applicability of the proposed model for interpretation of data from real foam tests.

Let us first interpret the data shown in Figure 1A, which were obtained by the foam rise method in the presence of Emulsion A with $C_{A0}=2\times10^{-4}$ g/cm^3. Since we still have no systematic data for the dependence of t^* on C_{A0}, we assume that $C_A^* << C_{A0}$. From the data shown in Figure 1A, one can determine $t^* \approx 2980$ s and $<C_B>=<V_F>/V_B \approx 390$ bubbles/cylinder. Then from Eqs. 9', 11, 13 and 14 one calculates $k_1 \approx 6500$ cm^3/(g.s), $k_2 \approx 1.7\times10^{-6}$ s^{-1}, $k_3 \approx 6.7\times10^{-8}$ g/(s.cm^3), and $Dr \approx 3.8\times10^9$

bubbles/(g/cm^3).

Since the experimental systems shown in Figures 1A and 1B are the same (only the foam test is different), one can assume that the constants k_1 and k_2 remain the same, whereas the rate of bubble generation, v_B, is different. From Figure 1B one can calculate t^*=30 N^*= 300 s. From the ratio $k_1/k_2 = (v_B t^*)/C_{A0}$ one can find v_B in the shake test to be about 2500 bubbles/s. This estimate is rather reasonable, because shake tests in the absence of antifoam showed that the rate of foam formation, $V_F \approx$ 150 cm^3/sec and the bubble diameter was around 5 mm.

Finally, we show in Figure 2 that the results from shake tests, performed at different durations of the shake cycle, fall in a single master curve when plotted as a function of the total duration of shaking (foaming). Note that these experiments are made with 0.01 wt % of Compound A (instead of 0.02 wt % of Emulsion A). From Figure 2B one sees that for this system $t^* \approx 910$ s. Assuming that v_B in these experiments was again ≈ 2500 bubbles/s (same as in Figure 1B), one can estimate for Compound A that $k_1 \approx 1.5\times10^5$ cm^3/(g.s), $k_2 \approx 6.7\times10^{-6}$ s^{-1}, $k_3 \approx 1.1\times10^{-7}$ g/(s.cm^3), and $Dr \approx 2.3\times10^{10}$ bubbles/(g/cm^3). The comparison of the respective values for k_1 and Dr indicates that Compound A is about 20 times more active and about 10 times more durable than Emulsion A.

4/ Conclusions.

- A phenomenological model for description of the performance of mixed PDMS-silica antifoams is proposed.
- According to the model, the most important characteristic of the foam test is the rate of bubble generation, v_B. In agreement with the experimental observations (3), one antifoam globule is assumed to rupture one foam film and, hence, to cause one bubble-bubble or bubble-atmosphere coalescence event. During the initial period, when the antifoam is very active (Stage 1), the rate of bubble coalescence is practically equal to the rate of bubble generation, v_B (steady-state approximation).
- The antifoam properties are described by three parameters: k_1, which characterizes the initial antifoam activity; k_2/k_1, which shows how rapidly the antifoam looses its activity in the course of foam destruction; and threshold antifoam concentration, C_A^*, below which the antifoam is unable to suppress efficiently the generated foam.
- The constants k_1 and k_2 are expected to depend slightly on the particular foam test. The threshold concentration C_A^*, in principle, could depend on the used foam test. In most practical cases, however, C_A^* is expected to be much smaller than the initial antifoam concentration, C_{A0}, and can be neglected.
- The model is supported by the results from several preliminary experiments with two different foam tests. More systematic experiments are currently under a way to verify the proposed model.

References:

1. Garrett, P. R., "The mode of action of antifoams"; In *Defoaming: Theory and Industrial Applications*, Garrett, P. R., Ed.; Marcel Dekker: New York, 1993; Chapter 1.
2. N. D. Denkov, K. Marinova, "Antifoaming action of oils", Proceedings 3rd Eurofoam Conference, June, 2000, Delft, The Netherlands; Verlag MIT Publishing, Bremen, 2000, pp. 199-206.
3. N. D. Denkov, P. Cooper, J.-Y. Martin, "Mechanisms of action of mixed solid-liquid antifoams. 1. Dynamics of foam film rupture", *Langmuir* **15** (1999) 8514.
4. N. D. Denkov, "Mechanisms of action of mixed solid-liquid antifoams. 2. Stability of oil bridges in foam films", *Langmuir* **15** (1999) 8530.
5. N. D. Denkov, K. Marinova, H. Hristova, A. Hadjiiski, P. Cooper, "Mechanisms of action of mixed solid-liquid antifoams. 3. Exhaustion and reactivation", *Langmuir* **16** (2000) 2515.
6. Hadjiiski, N. D. Denkov, S. Tcholakova, I. B. Ivanov, "Role of entry barriers in the foam destruction by oil drops", Proceedings 13th International Symposium on Surfactants in Solution, June, 2000, Gainsville, FL: Marcel Dekker: New York, 2002.